General scaling law for stiffness measurement of small bodies with applications to the atomic force microscope

John E. Sader[a)]
Department of Mathematics and Statistics, University of Melbourne, Victoria 3010, Australia

Jessica Pacifico
School of Chemistry, University of Melbourne, Victoria 3010, Australia

Christopher P. Green
Department of Mathematics and Statistics, University of Melbourne, Victoria 3010, Australia

Paul Mulvaney
School of Chemistry, University of Melbourne, Victoria 3010, Australia

(Received 8 February 2005; accepted 21 April 2005; published online 20 June 2005)

A general scaling law connecting the stiffness and dissipative properties of a linear mechanical oscillator immersed in a viscous fluid is derived. This enables the noninvasive experimental determination of the stiffness of small elastic bodies of arbitrary shape by measuring their resonant frequency and quality factor in fluid (typically air). In so doing, we elucidate the physical basis of the method of Sader *et al.* [Rev. Sci. Instrum. **70**, 3967 (1999)] for determining the stiffness of rectangular atomic force microscope cantilevers, and discuss its applicability. The validity of the derived general technique is demonstrated by calibrating atomic force microscope cantilevers with complex geometries, and its implications to small bodies in general are discussed. © *2005 American Institute of Physics*. [DOI: 10.1063/1.1935133]

I. INTRODUCTION

Force measurements at the nanometer scale are routinely performed using many techniques, which include optical tweezers,[1] surface forces apparatus,[2] and atomic force microscopy.[3] Arguably, the atomic force microscope (AFM) has emerged as the most versatile of these force-measuring techniques due to its ability to operate in ambient, liquid, and vacuous environments with nanometer spatial control and atomic-scale imaging resolution. Indeed, the AFM has found application in many areas of science and technology, ranging from the measurement of capillary forces at the microscopic scale[4] down to quantification of the mechanical properties of single molecules at the nanoscale.[5]

Fundamental to all such techniques is the ability to calibrate their force-sensing components, and thus enable conversion of the measured observables into an interaction force. While this is trivial for instrumentation that relies on macroscopic devices, such as the springs used in the surface forces apparatus,[2] those that use microscopic devices require special consideration since standard macroscopic techniques are often not suitable. This is nowhere more evident than in the determination of the stiffness of microcantilevers used in the AFM, which are some 100 microns in length. Importantly, microfabrication techniques often produce structures the material properties of which deviate significantly from bulk values.[6] Consequently, the use of bulk data to determine the mechanical characteristics of such structures is often not justified.

Stiffness determination of microcantilevers has been an area of significant research for more than ten years, with numerous techniques being developed.[7–12] These range from methods that utilize a static load to determine the stiffness[7–9] to methods that monitor the dynamic deflection properties of the cantilever.[10–12] Recently, Sader *et al.*[12] proposed a method to determine the spring constant (stiffness) of rectangular AFM cantilevers in a completely noninvasive fashion by measuring the resonant frequency and quality factor of the cantilever in fluid (such as air) and from the knowledge of its plan-view geometry. This method was derived using the results of a theoretical model for the frequency response of cantilever beams immersed in viscous fluids.[13] Importantly, this technique is restricted to a rectangular cantilever the length of which greatly exceeds its width, which in turn greatly exceeds its thickness, and is uniform along its entire length. The physical principle underpinning this method is yet to be described.

In this article, we show that the method of Sader *et al.*[12] is a subset of a general experimental technique enabling the stiffness of any small elastic body to be determined. In so doing, we elucidate the underlying physical basis of the method of Sader *et al.*,[12] discuss its applicability to rectangular cantilevers in the presence of nonidealities, and provide its rigorous extension to small elastic bodies of arbitrary shape. To demonstrate the validity of this general technique, the calibration of AFM cantilevers with complex geometries is investigated, since this can also be achieved using independent methods. We emphasize, however, that while such AFM cantilevers do not offer operational advantages over simple rectangular cantilevers,[14–16] the ability to calibrate their stiffness enables the accommodation of all current and future designs.

[a)]Author to whom correspondence should be addressed; electronic mail: jsader@unimelb.edu.au

More generally, microfabrication constraints often cause nonoptimal geometries to be adopted in micromechanical devices. Consequently, the ability to experimentally determine the stiffness of small bodies of arbitrary shape is of fundamental practical importance.

II. THEORY

We now derive the theoretical formalism for the general technique. To begin, we consider a linear harmonic oscillator with a single degree of freedom, the damping force of which is proportional to its velocity. If the oscillator is excited at its radial resonant frequency ω_R, then the quality factor Q of the oscillator is defined to be

$$Q = 2\pi \left. \frac{E_{\text{stored}}}{E_{\text{diss}}} \right|_{\omega=\omega_R}. \tag{1}$$

For oscillations of amplitude A, the energy stored in the oscillator $E_{\text{stored}} = \frac{1}{2} k A^2$, where k is the spring constant of the oscillator. E_{diss} is the energy dissipated per oscillation cycle. We note that for such a linear oscillator, the energy stored and the energy dissipated per cycle are both proportional to the square of the oscillation amplitude A. It then follows from Eq. (1) that the spring constant k of the oscillator is related to its dissipative properties by

$$k = \left(\frac{1}{2\pi} \left. \frac{\partial^2 E_{\text{diss}}}{\partial A^2} \right|_{\omega=\omega_R} \right) Q. \tag{2}$$

Since E_{diss} is proportional to the square of the oscillation amplitude A, Eq. (2) is independent of A.

Next, consider an elastic body immersed in a viscous (Newtonian) fluid, such as air, and for energy dissipation to occur predominantly in the fluid; for small bodies such as AFM cantilevers, this is the practical case. Provided the oscillation amplitude of the body is far smaller than any of its geometric length scales, the hydrodynamic force exerted by the fluid will be a linear function of the amplitude since the nonlinear convective inertial term in the Navier–Stokes equation is negligible in such cases. Consequently, the energy dissipated will be dependent on the square of the amplitude, as required. It then follows that the energy dissipated per oscillation cycle is only dependent on the fluid viscosity η, fluid density ρ, square of the amplitude A, length scale of the oscillator L_0, its radial resonant frequency ω_R in fluid, its mode shape at resonance, and geometry. Note that the last two properties are dimensionless quantities.

The functional form of E_{diss} for such a body, in relation to these parameters, can be rigorously determined using dimensional analysis.[17] It follows that the product

$$\rho^m \eta^n L_0^p \omega_R^q \left(\frac{1}{2\pi} \left. \frac{\partial^2 E_{\text{diss}}}{\partial A^2} \right|_{\omega=\omega_R} \right), \tag{3}$$

must be dimensionless, where m, n, p, and q are constants to be determined. Equating dimensions in Eq. (3) leads to two independent dimensionless groups:

$$\Pi \equiv \frac{1}{\rho L_0^3 \omega_R^2} \left(\frac{1}{2\pi} \left. \frac{\partial^2 E_{\text{diss}}}{\partial A^2} \right|_{\omega=\omega_R} \right), \quad \text{Re} \equiv \frac{\rho L_0^2 \omega_R}{\eta}. \tag{4}$$

The latter parameter Re is commonly referred to as the Reynolds number.[13]

From Buckingham's theorem,[17] it then follows that there must exist a function H such that

$$H\left(\frac{1}{\rho L_0^3 \omega_R^2} \left(\frac{1}{2\pi} \left. \frac{\partial^2 E_{\text{diss}}}{\partial A^2} \right|_{\omega=\omega_R} \right), \quad \frac{\rho L_0^2 \omega_R}{\eta} \right) = 0, \tag{5}$$

which relates the energy dissipated per cycle E_{diss} to all other parameters. Solving Eq. (5) for the first argument and rearranging gives

$$\left. \frac{1}{2\pi} \frac{\partial^2 E_{\text{diss}}}{\partial A^2} \right|_{\omega=\omega_R} = \rho L_0^3 \omega_R^2 \Omega(\text{Re}), \tag{6}$$

where the dimensionless function $\Omega(\text{Re})$ is to be determined.

Substituting Eq. (6) into Eq. (2) then gives

$$k = \rho L_0^3 \Omega(\text{Re}) \omega_R^2 Q. \tag{7}$$

Equation (7) is the result we seek, and relates the stiffness of the body to its resonant frequency, quality factor, geometry, and the properties of the fluid. We emphasize that the dimensionless function $\Omega(\text{Re})$ also implicitly depends on the geometry and deflection function of the body, which are also dimensionless. This function can be determined either theoretically or experimentally, as we shall discuss below. Importantly, once it is determined for a body of given size as a function of Re, the function then holds universally for bodies of the same geometry, but different size.

The resonant frequency ω_R and quality factor Q can be measured by fitting the frequency response of the body to the response of a simple harmonic oscillator.[12,18] This implicitly requires the damping coefficient of the oscillator to be independent of frequency. Since the hydrodynamic damping coefficient of an arbitrary body is frequency dependent in general, but only weakly so,[19] it follows that the fundamental-mode resonance peak must be sharp and narrow so that the damping coefficient is constant in the neighborhood of the peak, i.e., the quality factor must greatly exceed unity. This also enables the motion of the body to be described by a linear harmonic oscillator with a single degree of freedom, as has been assumed. This fundamental condition that the quality factor greatly exceed unity must, therefore, also be satisfied by Eq. (7) in general. This condition can be relaxed in cases where the damping coefficient can be determined to be independent of frequency, e.g., this is expected when the Reynolds number Re is far smaller than unity.

We restrict our discussion in this article to the fundamental mode of the body, although we note that Eq. (7) can be applied to any oscillation mode.

III. RESULTS AND DISCUSSION

A. Rectangular AFM cantilevers

Equation (7) is to be compared against the formula of Sader *et al.*,[12] which we now briefly review. Under the assumptions that the cantilever is (i) of rectangular geometry,

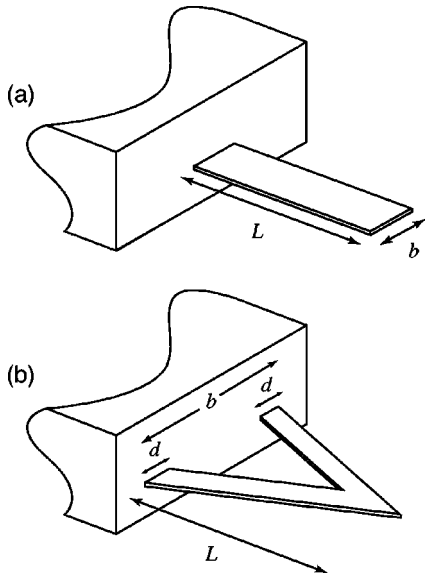

FIG. 1. Schematic illustration showing the plan-view dimensions of a (a) rectangular cantilever and a (b) V-shaped cantilever.

(ii) immersed in a viscous fluid, (iii) its length L greatly exceeds its width b, which in turn greatly exceeds its thickness, (iv) uniform along its entire length, and (v) its quality factor greatly exceeds unity, Sader *et al.*[12] derived the formula

$$k = 0.1906\ \rho b^2 L \Gamma_i(\omega_R)\omega_R^2 Q, \tag{8}$$

which connects the normal spring constant k of the cantilever to its fundamental-mode resonant frequency ω_R and quality factor Q in fluid, length L, width b, fluid viscosity η, and fluid density ρ. A schematic of a rectangular cantilever showing the dimensions is given in Fig. 1. The function Γ_i is the imaginary part of the hydrodynamic function derived in Ref. 13, and depends only on the Reynolds number Re. An analogous result for the torsional spring constant is presented in Ref. 20.

Importantly, Eq. (8) is identical in form to Eq. (7), which establishes that the method of Sader *et al.*[12] is a subset of the more general class of method defined by Eq. (7). Since the length scale of the hydrodynamic flow around an oscillating rectangular cantilever is given by its width, we choose $L_0 = b/2$ (in line with Ref. 13). It follows that

$$\Omega(\mathrm{Re}) = 1.525\frac{L}{b}\Gamma_i(\omega_R), \tag{9}$$

where $\mathrm{Re} = \rho b^2 \omega/(4\eta)$. This analysis also establishes that the term $0.1906\ \rho b^2 L \Gamma_i(\omega_R)\omega_R^2$ in Eq. (8) is connected directly to the energy dissipated per cycle E_{diss}, namely,

$$\frac{1}{2\pi}\frac{\partial^2 E_{\mathrm{diss}}}{\partial A^2}\bigg|_{\omega=\omega_R} = 0.1906\ \rho b^2 L \Gamma_i(\omega_R)\omega_R^2. \tag{10}$$

These findings have important practical consequences, as we shall now discuss. For a thin cantilever, i.e., one whose width and length greatly exceed its thickness, the energy dissipated in the fluid is only dependent on its plan-view geometry and deflection function, since the flow around the cantilever is not influenced by its thickness. Consequently, if the thickness of the cantilever is not uniform over its entire length, in violation of condition (iv) above, but the deflection function is approximately the same as that of a uniform cantilever, then the energy dissipated per cycle of both cantilevers will have approximately the same functional form.

This establishes that Eq. (8) holds for cantilevers of uniform and nonuniform thickness, provided the deflection function of the cantilever is approximately the same as that of a cantilever of uniform thickness. Importantly, thickness variations exert only a weak effect on the fundamental-mode deflection function, which, in general, closely resembles that of a cantilever under static load at its end tip, i.e., a monotonically increasing displacement as a function of distance from the clamped end.

In addition, this explains the recent experimental result of Green *et al.*,[20] which demonstrated that Eq. (8) also holds for cantilevers that are loaded with spheres at their end tips. In that study, it was found that the validity of Eq. (8) in application to a sphere-loaded cantilever depends only on the size of the sphere, not its mass. Significant discrepancies were observed only when the size of the sphere became comparable to the width of the cantilever, in which case Eq. (8) underestimated the true spring constant. This phenomenon can now be easily understood. First, we note that the deflection function of an unloaded cantilever of uniform thickness is approximately identical to that of the same cantilever with an arbitrary point mass added to its end tip.[21] It therefore follows that Eq. (8) is also valid for sphere-loaded cantilevers, provided the added sphere does not affect the energy dissipated per cycle, which is certainly true when the sphere diameter is far smaller than the cantilever width, i.e., the hydrodynamic length scale. However, when the sphere diameter becomes comparable to or exceeds the width of the cantilever, it affects the flow around the cantilever, enhancing the energy dissipated per cycle. Consequently, in such a case, Eq. (10) will underestimate the true energy dissipated, leading to an underestimation of the spring constant by Eq. (8), as observed in Ref. 20.

B. Experimental determination of $\Omega(\mathrm{Re})$

We now describe how the dimensionless function $\Omega(\mathrm{Re})$ can be determined for a body of arbitrary geometry and composition. In principle, $\Omega(\mathrm{Re})$ can be calculated theoretically for any body by solving the coupled fluid–structure interaction problem and making use of Eq. (7). However, this poses a formidable challenge in all but the simplest geometries, thus necessitating the use of numerical techniques. Nonetheless, since $\Omega(\mathrm{Re})$ depends only on the Reynolds number Re and the geometry of the body, it can be easily determined experimentally for a single body by adjusting Re, as we shall discuss below. Once $\Omega(\mathrm{Re})$ is found for that single body, then it holds true for all such bodies with the same geometry, even if the size and composition are varied, provided the deflection function and mode are identical.

To undertake this experimental procedure, we first require the stiffness of the single body for which the dimensionless function $\Omega(\mathrm{Re})$ is to be determined; this can be determined either theoretically or by using an independent

TABLE I. Dimensions of the cantilevers used in this study (Microlever, Veeco, USA). Geometric parameters are shown in Fig. 1. All cantilevers are coated with gold with a nominal thickness of 50 nm by the manufacturer. The total thickness of the cantilevers is nominally 0.6 μm. Spring constants k measured using the method in Ref. 12.

Cantilever	L (μm)	b (μm)	d (μm)	k (N m^{-1})
R	200	20	⋯	0.020
V_1	320	215	21	0.013
V_1	220	150	21	0.038

experimental technique. $\Omega(\mathrm{Re})$ can then be evaluated as a function of Re by immersing the body in gas, such as air, adjusting the gas pressure, and making use of Eq. (7). This allows for the determination of $\Omega(\mathrm{Re})$ over many orders of magnitude in Re, since gas density is proportional to pressure; gas viscosity is independent of pressure and the resonant frequency is typically a very weak function of pressure. We emphasize, however, that this procedure is only valid provided the mean free path of the gas does not become comparable to or larger than the length scale of the body. If this condition is violated, then the underlying continuum assumption in the analysis will be invalid.

To illustrate the validity of this approach, we present measurements on a *rectangular* AFM cantilever, cantilever R in Table I [Microlever, Veeco, USA], and compare these results to the known analytical solution, Eq. (9), for $\Omega(\mathrm{Re})$. The stiffness of the cantilever was measured using the method of Sader *et al.*[12] at atmospheric pressure and was determined to be 0.020 N/m. Choosing the length scale of the cantilever to be its half width $L_0=b/2$, as in Ref. 13, Eqs. (4) and (7) then yield the following expressions:

$$\Omega(\mathrm{Re})=\frac{8k}{\rho b^3\omega_R^2 Q},\quad \mathrm{Re}=\frac{\rho b^2\omega_R}{4\eta}. \tag{11}$$

The resonant frequency ω_R and quality factor Q of the cantilever were determined by measuring its thermal noise spectrum. This was performed using a National Instruments data acquisition (DAQ) card,[22] amplifying the photodiode signal using a wideband (1 MHz) amplifier with a low-frequency roll-off to remove dc noise, and finally carrying out a digital fast Fourier transform of the signal using the LABVIEW software.[23] The fundamental resonance peak was fitted to the response of a simple harmonic oscillator[18] using a nonlinear least-squares-fitting procedure.[24] A white-noise floor was included in the fitting procedure[12] to ensure accurate fits to the measured data. The gas pressure surrounding the cantilever was varied by placing the entire AFM into a specially constructed bell jar, adapted so the photodiode voltage and AFM control leads could be fed through the base. The bell jar was evacuated on a vacuum line, and results were obtained for pressures ranging from 760 Torr (1 atm) down to 3 Torr, at which point the mean free path of the gas became comparable to the cantilever width. All measurements were performed at a temperature of 27 °C. Results showing the measured resonant frequencies and quality factors as functions of air pressure are shown in Fig. 2.

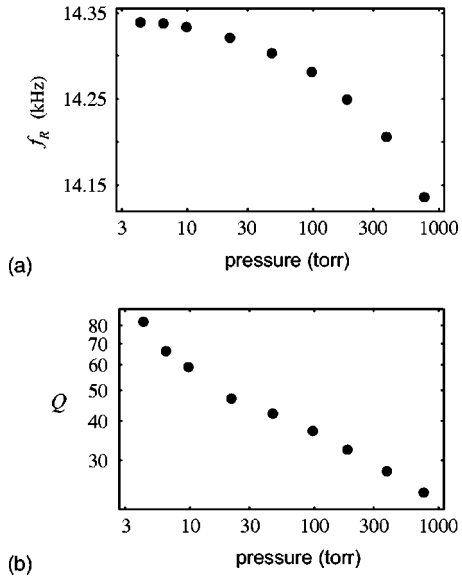

FIG. 2. Measured (a) resonant frequencies $f_R=\omega_R/(2\pi)$ and (b) quality factors of a rectangular cantilever R as a function of air pressure.

In Fig. 3, we present a comparison of the theoretical solution, Eq. (9), to the experimental measurement of $\Omega(\mathrm{Re})$ obtained by substituting the results of Fig. 2 into Eq. (11). It is strikingly evident that measurements and theory show excellent agreement over the entire range of Re presented, thus validating the procedure. In passing, we note that for cases where the mean free path was larger than the cantilever width, the measured $\Omega(\mathrm{Re})$ underestimated the theoretical $\Omega(\mathrm{Re})$, as would be expected since substantial slip is present at the cantilever surface in such cases.

To increase Re above the value obtained at atmospheric pressure requires the medium surrounding the cantilever to be pressurized. If this is not feasible, then the use of a gas with a kinematic viscosity η/ρ smaller than that of air at 760 Torr will achieve identical results. To illustrate this approach, the rightmost data point in Fig. 3 was obtained using carbon dioxide, which has a kinematic viscosity approximately half that of air at 760 Torr, namely, $(\eta/\rho)_{\mathrm{CO_2}}=0.83\times10^{-5}$ m^2 s^{-1}, whereas $(\eta/\rho)_{\mathrm{air}}=1.58\times10^{-5}$ m^2 s^{-1}. All other data points were obtained in air. As is clear from Fig. 3, the data point obtained using carbon dioxide matches the trend obtained using air, and shows excellent agreement with the analytical solution.

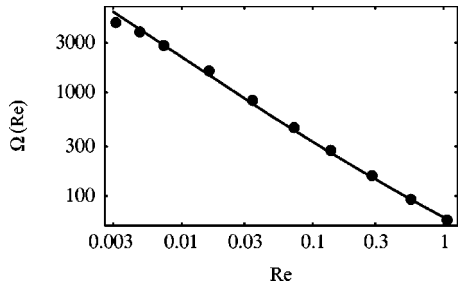

FIG. 3. Dimensionless function $\Omega(\mathrm{Re})$ for rectangular cantilever R. Measurements shown as solid circles. The solid line corresponds to theoretical result, Eq. (9).

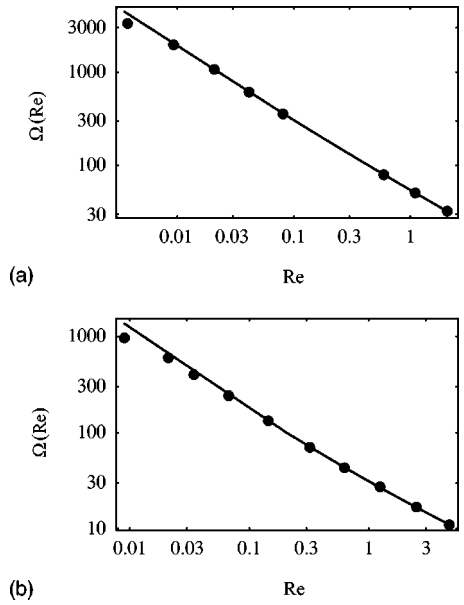

FIG. 4. Dimensionless functions $\Omega(\mathrm{Re})$ for V-shaped cantilevers: (a) V_1, (b) V_2. Measurements are shown as solid circles. The solid lines are corresponding fits to the measured data points, with empirical formulas given by (a) $\Omega(\mathrm{Re})=54.33\mathrm{Re}^{-0.728+0.00915\ \ln \mathrm{Re}}$ and (b) $\Omega(\mathrm{Re})=31.14\mathrm{Re}^{-0.700+0.0215\ \ln \mathrm{Re}}$.

C. Validation of the general technique

We now demonstrate the validity of the new general technique by applying it to the calibration of AFM cantilevers with complex geometries, since the stiffness of these bodies can be easily determined by independent means. The cantilevers used have V-shaped geometries,[14–16] and thus preclude direct usage of Eq. (8), which is valid for rectangular cantilevers only. These cantilevers were chosen as test cases, since they were on the same chip as the rectangular cantilever used in the previous section, allowing for the immediate and accurate determination of their spring constants using the independent approach discussed in Sec. IV of Ref. 12. The geometries, dimensions, and spring constants of these V-shaped cantilevers are given in Fig. 1 and Table I. These cantilevers are composed of silicon nitride and are gold coated with a nominal thickness of 50 nm by the manufacturer.

To begin, the dimensionless function $\Omega(\mathrm{Re})$ of these cantilevers was measured using the experimental procedure detailed in the previous section, the results of which are given in Fig. 4. The length scale of both cantilevers was taken to be their arm widths, i.e., $L_0=d$. A comparison with theory is not possible, since no analytical solution to $\Omega(\mathrm{Re})$ is known for these geometries. Nonetheless, we note that $\Omega(\mathrm{Re})$ for both cantilevers possess similar functional forms to each other and to that of the rectangular cantilever, cf. Figs. 3 and 4. To aid implementation of these results, an empirical function for $\Omega(\mathrm{Re})$ was fitted to the data and presented in the caption of Fig. 4. Substituting these empirical fits into Eq. (7) results in explicit formulas for the spring constants of these two types of cantilevers,[25] which are valid provided the Reynolds number Re lies within the range specified in Fig. 4,

$$V_1: \quad k = 3.57\rho d^2 L \mathrm{Re}^{-0.728+0.00915\ \ln \mathrm{Re}}\omega_R^2 Q, \tag{12a}$$

$$V_2: \quad k = 2.97\rho d^2 L \mathrm{Re}^{-0.700+0.0215\ \ln \mathrm{Re}}\omega_R^2 Q, \tag{12b}$$

where

$$\mathrm{Re} = \frac{\rho d^2 \omega_R}{\eta}. \tag{13}$$

We emphasize that while these formulas were obtained using single cantilevers, they are universally applicable to cantilevers with the same geometries, irrespective of their composition and thickness. To illustrate this property, below we determine the spring constants of the V-shaped cantilevers of Green *et al.*[20] using Eqs. (12) and compare these results to the spring constants determined in Ref. 20. Importantly, the cantilevers used by Green *et al.*[20] have identical plan-view geometries to the present cantilevers, but are not coated with gold. Consequently, Eqs. (12a) and (12b) are also expected to hold for these cantilevers, as discussed above. All measurements were performed at 760 Torr. Note that if cantilevers of different geometries are used in place of those specified in this article, then the dimensionless function $\Omega(\mathrm{Re})$ should be re-evaluated.

In Table II we present the results for the resonant frequencies, quality factors, and spring constants k_{prev} of the uncoated V-shaped cantilevers, as measured by Green *et al.*[20] We also evaluate the spring constants of these cantilevers by directly substituting their resonant frequencies and quality factors into Eqs. (12). These newly measured spring constants, denoted k_{new}, are to be compared to k_{prev}, where excellent agreement is found, thus illustrating the validity of the new method. We emphasize that the resonant frequencies and quality factors of the coated and uncoated cantilevers differ significantly (see Table II), yet the new method accommodates these differences naturally.

Next, we modified the spring constants of the gold-coated cantilevers used in this study in order to assess the validity of the method for changing cantilever stiffness. A similar, but different, chip from the same wafer was used in place of the one from which the results in Fig. 4 were obtained. The spring constants were modified by depositing additional gold using a sputter coater; this modified the cantilever mass and rigidity. Gold of identical thickness was deposited on both sides of the cantilever to minimize bending that would, otherwise, result if gold were only deposited on one side. Since the rectangular and V-shaped cantilevers

TABLE II. Table showing the comparison of spring constants for uncoated V-shaped cantilevers used by Green *et al.* (Ref. 20) k_{prev} refers to results presented in Ref. 20, whereas k_{new} corresponds to the new method obtained using Eqs. (12) and $f_R=\omega_R/(2\pi)$. These results are to be compared against the gold-coated cantilevers specified in Table I: Cantilever V_1 ($f_R=6.29$ kHz, $Q=15.1$), cantilever V_2 ($f_R=14.17$ kHz, $Q=26.0$); spring constants are identical to the uncoated cantilevers. All measurements are performed at 760 Torr. Properties of air: $\rho=1.18\ \mathrm{kg\,m^{-3}}$ and $\eta=1.86\times10^{-5}\ \mathrm{kg\,m^{-1}\,s^{-1}}$.

Cantilever	f_R (kHz)	Q	k_{prev} ($\mathrm{N\,m^{-1}}$)	k_{new} ($\mathrm{N\,m^{-1}}$)
V_1	7.82	10.6	0.013	0.012
V_2	18.77	19.1	0.038	0.040

TABLE III. Table showing the comparison of spring constants for varying additional gold-coating thickness. k_{prev} refers to the results obtained using the previous method in Ref. 12, whereas k_{new} corresponds to the new method, Eqs. (12) and $f_R=\omega_R/(2\pi)$. For the rectangular cantilever *R*, the new and previous methods are identical, since the dimensionless function $\Omega(\mathrm{Re})$ is known theoretically. The nominal thickness of all unmodified cantilevers is 0.6 μm. All measurements are performed at 760 Torr. Properties of air: $\rho=1.18\ \mathrm{kg\,m^{-3}}$ and $\eta=1.86\times10^{-5}\ \mathrm{kg\,m^{-1}\,s^{-1}}$.

Cantilever	Gold thickness (nm)	f_R (kHz)	Q	k_{prev} (N m^{-1})	k_{new} (N m^{-1})
R	0	14.05	23.8	0.020	···
R	120	11.36	38.2	0.025	···
R	342	10.57	67.3	0.040	···
R	430	10.87	81.3	0.050	···
V_1	0	6.27	15.7	0.013	0.013
V_1	120	5.08	25.5	0.016	0.017
V_1	342	4.81	43.3	0.026	0.027
V_1	430	4.88	54.0	0.032	0.034
V_2	0	14.27	24.0	0.038	0.035
V_2	120	11.60	45.1	0.046	0.050
V_2	342	10.94	78.3	0.075	0.080
V_2	430	11.38	90.0	0.093	0.097

are adjacent to each other on the same chip, we were able to determine the thickness of gold deposited and the change in stiffness of all cantilevers from the measurements of the rectangular cantilever. The stiffness of the rectangular cantilever was measured using Eq. (8), and the thickness of gold was determined using Eq. (3) of Ref. 12, which only requires the resonant frequency and quality factor of the cantilever and the density of gold. The stiffness of the adjacent V-shaped cantilevers could then be determined using the approach in Sec. IV of Ref. 12; the thickness of gold on all cantilevers was identical due to the proximity of the cantilevers.

Results of this comparison are shown in Table III for the rectangle and two V-shaped cantilevers. We note that the thickness, mass, and spring constant of all cantilevers are modified significantly by the deposited gold. Initially, the resonant frequency decreases due to the increase in mass, and eventually increases due to the enhanced stiffness, as expected.[6] The quality factors of all cantilevers increase as gold is deposited. Despite the dramatic changes in resonant frequency, quality factor, and stiffness, the results in Table III demonstrate the validity of the new method in accurately predicting the change in spring constant of the V-shaped cantilevers.

Finally, we assess the validity of the new method when masses are attached to the end tips of the cantilevers, as is often encountered in practice. For this purpose, we used one of the V-shaped cantilevers studied in Ref. 20 with identical plan-view geometry to cantilever V_2 and applied the new general method. Results of this comparison are presented in Table IV for the addition of tungsten spheres of varying diameter. Adding a mass to the end of the cantilever does not modify its spring constant, but can significantly affect both its resonant frequency and quality factor. Provided the sphere does not significantly modify the functional form of the hydrodynamic load, the dimensionless function $\Omega(\mathrm{Re})$ measured for the unloaded cantilever will remain unchanged and the method valid. As for the rectangular cantilevers studied in Ref. 20 using the method of Sader *et al.*,[12] we find that adding a sphere to the V-shaped cantilever reduces the measured spring constant. Nonetheless, the new method remains valid, provided the sphere diameter is not comparable to the hydrodynamic length scale of the cantilever, i.e., its arm width. This is as expected, since a sphere comparable to the hydrodynamic length scale can significantly modify the hydrodynamic load, and thus enhance the energy dissipated per cycle by the cantilever. This leads to Eq. (12b) underestimating the true energy dissipated per cycle, and consequently an underestimation of the spring constant by the new method.

TABLE IV. Table showing the effect of added mass on the validity of the new method, Eq. (12b), for the uncoated V-shaped cantilever in Ref. 20 with geometry identical to cantilever V_2. The measured spring constant of the cantilever is 0.039 N/m. Tungsten spheres of varying diameter were used. All measurements were performed at 760 Torr. Properties of air: $\rho=1.18\ \mathrm{kg\,m^{-3}}$ and $\eta=1.86\times10^{-5}\ \mathrm{kg\,m^{-1}\,s^{-1}}$.

Sphere diameter (μm)	f_R (kHz)	Q	k_{new} (N m^{-1})
0	17.99	19.4	0.039
7	11.92	33.0	0.038
9	10.59	37.9	0.037
10	9.35	43.2	0.036
12	6.92	56.5	0.032
14	5.52	66.6	0.028

IV. CONCLUSIONS

We have presented a general scaling law enabling the measurement of the stiffness of small bodies of arbitrary geometry and composition. All that is required is the determination of the dimensionless function $\Omega(\mathrm{Re})$, which may be achieved theoretically or experimentally on a single body by adjusting the surrounding gas pressure. The resulting dimensionless function $\Omega(\mathrm{Re})$ will then be valid for all such bodies of identical geometry, regardless of their size and composition, provided the energy dissipated is dependent only on the density and viscosity of the surrounding medium. To illustrate the validity of the technique, measurements were performed on two types of V-shaped AFM cantilevers. The new technique thus extends the method of Sader *et al.*[12] to small elastic bodies of arbitrary shape, allowing for the noninvasive calibration of their stiffness. This is expected to be of value to users of the AFM, and for the general calibration of small-scale mechanical devices and structures.

ACKNOWLEDGMENTS

This research was supported by the Particulate Fluids Processing Centre of the Australian Research Council and by the Australian Research Council Grants Scheme. J.P. thanks the Swiss NSF for support through Grant No. PBNE2-102378.

[1] J. C. Crocker and D. G. Grier, J. Colloid Interface Sci. **179**, 298 (1996).
[2] J. N. Israelachvili and G. E. Adams, J. Chem. Soc., Faraday Trans. 1 **74**, 975 (1978).

[3]G. Binnig, C. F. Quate, and Ch. Gerber, Phys. Rev. Lett. **56**, 930 (1986).
[4]B. Cappella and G. Dietler, Surf. Sci. Rep. **34**, 1 (1999).
[5]M. Rief, M. Gautel, F. Oesterhelt, J. M. Fernandez, and H. E. Gaub, Science **276**, 1109 (1997).
[6]J. E. Sader, I. Larson, P. Mulvaney, and L. R. White, Rev. Sci. Instrum. **66**, 3789 (1995).
[7]H.-J. Butt *et al.*, J. Microsc. **169**, 75 (1993).
[8]T. J. Senden and W. A. Ducker, Langmuir **10**, 1003 (1994).
[9]A. Torii, M. Sasaki, K. Hane, and S. Okuma, Meas. Sci. Technol. **7**, 179 (1996).
[10]J. P. Cleveland, S. Manne, D. Bocek, and P. K. Hansma, Rev. Sci. Instrum. **64**, 403 (1993).
[11]J. L. Hutter and J. Bechhoefer, Rev. Sci. Instrum. **64**, 1868 (1993).
[12]J. E. Sader, J. W. M. Chon, and P. Mulvaney, Rev. Sci. Instrum. **70**, 3967 (1999); online implementation of this method can be found at http://www.ampc.ms.unimelb.edu.au/afm
[13]J. E. Sader, J. Appl. Phys. **84**, 64 (1998).
[14]T. R. Albrecht, S. Akamine, T. E. Carver, and C. F. Quate, J. Vac. Sci. Technol. A **8**, 3386 (1990).
[15]J. E. Sader, Rev. Sci. Instrum. **74**, 2438 (2003).
[16]J. E. Sader and R. C. Sader, Appl. Phys. Lett. **83**, 3195 (2003).
[17]P. W. Bridgman, *Dimensional Analysis* (Yale University Press, New Haven, 1931).
[18]The radial resonant frequency ω_R and the quality factor Q are obtained by fitting the power spectrum in fluid to the function $B\omega_R^4/[(\omega^2-\omega_R^2)^2+\omega^2\omega_R^2/Q^2]$, where ω is the radial frequency. The fitting parameters are B, ω_R, and Q.
[19]This dependence is weak and varies approximately as the square root of the oscillation frequency at most (Ref. 13)
[20]C. P. Green, H. Lioe, J. P. Cleveland, R. Proksch, P. Mulvaney, and J. E. Sader, Rev. Sci. Instrum. **75**, 1988 (2004).
[21]For an added point mass that greatly exceeds the cantilever mass, the deflection function of the fundamental mode of vibration is identical to that of a statically loaded cantilever.
[22]AT-MIO-16E-1 board, available from National Instruments, 6504 Bridge Point Parkway, Austin, TX 78730-5039.
[23]LABVIEW is a registered trademark of, and is available from, National Instruments, see Ref. 22.
[24]MATHEMATICA is a registered trademark of, and is available from, Wolfram Research, Inc., 100 Trade Center Drive, Champaign, IL 61820-7237.
[25]The dimensionless function $\Omega(\mathrm{Re})$ was scaled by the arm width ratio L/d, as for the rectangular cantilever.